

## SUPPLEMENTARY MATERIAL TO:

### Paleozoic evolution of western Marie Byrd Land, Antarctica

Chris Yakymchuk\*, Caitlin R. Brown, Michael Brown, Christine S. Siddoway, C. Mark Fanning, Fawna J. Korhonen

**Figure DR1: Map of the Ford Ranges with U–Pb ages of Devonian–Carboniferous rocks**

**Table DR1: Sample Locations**

**Table DR2: Major element, trace element and REE concentrations**

**Table DR3: Sr–Nd isotope compositions**

**Table DR4: Summary of SHRIMP U–Pb results for zircon.**

**Table DR5: Summary of LA-ICP-MSP U-Pb results for zircon**

**Table DR6: U–Pb data for detrital zircon analyses**

**Table DR7: Whole-rock oxygen isotope results**

**Table DR8: Hf isotope analyses for detrital zircons**

**Table DR9: Hf and O isotope analyses of zircons from igneous rocks**

**Table DR10: *p* values for Kruskal-Wallis test of zircon  $\epsilon\text{Hf}_t$  and  $\delta^{18}\text{O}$  distributions**

## SAMPLE LOCATIONS

The coordinates and names of sample localities are shown in Table DR1.

## ANALYTICAL METHODS

### Major oxide, trace element and REE chemistry

Major oxide and select trace elements were analyzed by X-ray fluorescence spectrometry at Franklin and Marshall College. A PANanalytical 2404 X-ray fluorescence vacuum spectrometer equipped with a PW2540 X-Y sample handler was used following the procedures described by Boyd and Mertzman (1987). FeO was analyzed by  $\text{Fe}^{2+}$  titration and the  $\text{Fe}_2\text{O}_3$  was calculated by difference.

Rare earth elements were analyzed by inductively coupled plasma mass spectrometry at the University of Maryland. Twenty milligrams of powdered sample was dissolved in closed Savillex® Teflon beakers using 0.5 ml of 14M  $\text{HNO}_3$  and 3 ml of 29M HF. Samples were digested for 24 hours, dried down and subjected to a second dissolution in 0.25 ml 12M  $\text{HClO}_4$ , 0.5 ml of 14M  $\text{HNO}_3$  and 3 ml of 29M HF for 72 hours. The solution was dried down, brought up in 6M HCl and dissolved for an additional 24 hours; this last procedure was repeated until the sample was fully dissolved. Samples were diluted by a factor of 100. One ml of a 20 ppb  $^{115}\text{In}$  solution was added to the diluted sample to enable correction for instrumental drift.

The isotopes  $^{115}\text{In}$ ,  $^{139}\text{La}$ ,  $^{140}\text{Ce}$ ,  $^{141}\text{Pr}$ ,  $^{143}\text{Nd}$ ,  $^{147}\text{Sm}$ ,  $^{153}\text{Eu}$ ,  $^{158}\text{Gd}$ ,  $^{159}\text{Tb}$ ,  $^{163}\text{Dy}$ ,  $^{165}\text{Ho}$ ,  $^{167}\text{Er}$ ,  $^{169}\text{Tm}$ ,  $^{173}\text{Yb}$  and  $^{175}\text{Lu}$  were analyzed using a Finnigan Element 2 single collector ICP-MS; solutions were introduced into the plasma using an APEX desolvating nebulizer. USGS standards G-2, a granite, and MAG-1, a marine sediment, were used to calculate sample concentrations. Signals were corrected for instrumental drift, by normalizing all data to the  $^{115}\text{In}$  signal in the G-2 standard, and the blank, which was <0.1% of the signal for standards and <0.7% of the signal for unknowns. Granites and orthogneisses were corrected using USGS standard G-2, while metasedimentary and paragneiss samples were corrected using USGS standard MAG-1. Uncertainties from counting statistics ranged from 1% to 6%, and propagated uncertainties for concentrations ranged from 4% to 12%. The analytical data are reported in Table DR2.

### Whole-rock geochemical compositions (University of Maryland)

Sr and Nd isotope compositions were determined in the Isotope Geochemistry Laboratory at the University of Maryland. The rocks were prepared in a manner similar to that of Korhonen et al. (2010). Fifty milligrams of sample powder were dissolved in Savillex® Teflon beakers using 3 ml of 29M HF and 0.5 ml of 14M  $\text{HNO}_3$ . Isotopic spikes enriched in  $^{87}\text{Rb}$ ,  $^{84}\text{Sr}$ ,  $^{149}\text{Sm}$ , and  $^{150}\text{Nd}$  were added to powdered samples and underwent closed vessel digestion at 180–190°C for 24 hours. Samples were dried and re-dissolved in 3 ml of 29M HF, 0.5 ml of 14M  $\text{HNO}_3$ , and 0.25 ml of 12M  $\text{HClO}_4$ , and digested for a further 72 hours at 180–190°C, then dried. To finish, 2 ml of 6M HCl was added to the samples, which were digested at 180°C for 24 hours and dried again; this last procedure was repeated until the resulting solution was clear, after which samples were finally dried and brought up in 2 ml of 2.5M HCl.

Rubidium, Sr and REEs were separated from each other using a primary cation exchange column using AG50Wx4 (200–400 mesh) resin. Samples were loaded into column in chloride

form. Rubidium and Sr were eluted from the column in 2.5M HCl, while the REE were eluted in 6M HCl. Rubidium cuts were dried and diluted in 2% HNO<sub>3</sub>. Strontium cuts were passed through a cleanup column using Eichrom™ Sr-spec resin and eluted in 0.05M HNO<sub>3</sub>. The REE cuts from the primary column were passed through a secondary column using AG50Wx4 (200–400 mesh) resin. Samarium and Nd were eluted in 0.225M methyllactic acid (pH = 4.67).

Strontium, Nd and Sm ratios were analyzed using a VG Sector 54 TIMS. Strontium cuts were loaded onto a single Re filament with a Ta-oxide activator, and analyzed in a multi-dynamic mode. Strontium isotopes were corrected for mass fractionation by normalizing the measured <sup>87</sup>Sr/<sup>86</sup>Sr ratio to the <sup>86</sup>Sr/<sup>88</sup>Sr ratio = 0.1194. Repeated analysis of SRM 987 during the course of this study yielded an average <sup>87</sup>Sr/<sup>86</sup>Sr value of 0.710238 (n = 30). The mass fractionation corrected and spike corrected <sup>87</sup>Sr/<sup>86</sup>Sr ratio was normalized the average SRM 987 <sup>87</sup>Sr/<sup>86</sup>Sr value to correct for instrumental bias. Strontium blank concentrations averaged 14.0 ng (n = 4), <1% of sample Sr concentrations.

Rubidium ratios were measured using a Nu Plasma multi-collector (MC) ICP-MS at the University of Maryland. Samples were diluted by a factor of 100 and were introduced into the plasma using an Aridus I desolvating nebulizer. A 50 ppb Rb SpecPure® plasma standard was introduced after every three sample analyses and was used to correct for instrumental fractionation and drift. Rubidium blanks averaged 8.04 ppm (n = 4), <1% of the sample Rb concentrations.

Neodymium and Sm were loaded on two Re filaments with phosphoric acid and loaded in a triple filament arrangement. Neodymium ratios were measured in dynamic mode and corrected for mass fractionation by normalizing the measured <sup>143</sup>Nd/<sup>144</sup>Nd ratio to <sup>146</sup>Nd/<sup>144</sup>Nd = 0.7219. Repeated analysis of the Ames standard during the course of this study yielded an average <sup>143</sup>Nd/<sup>144</sup>Nd value of 0.512126 (n = 33). The fractionation and spiked corrected <sup>143</sup>Nd/<sup>144</sup>Nd ratio was normalized to the average Ames <sup>143</sup>Nd/<sup>144</sup>Nd value to correct for instrumental bias. Samarium was measured in static mode. Samarium blanks averaged 0.311 ng (n = 3) while Nd blanks averaged 2.28 ng (n = 3); both <1% of sample Sm and Nd concentrations.

The USGS G-2 granite was analyzed 7 times over a period of 12 months. Repeat analyses yielded an average <sup>87</sup>Sr/<sup>86</sup>Sr of 0.709767 ± 0.000038 (n = 7) and an average <sup>143</sup>Nd/<sup>144</sup>Nd of 0.512243 ± 0.000010 (n = 7). Rubidium concentrations averaged 167.6 ppm (range 162.9–174.2 ppm), Sr concentrations 488.8 ppm (range 482.1–496.2 ppm), and Rb/Sr ratios ranged from 0.3367 to 0.3511. Samarium concentrations averaged 7.1 ppm (range 7.0–7.3 ppm), Nd concentrations 52.6 ppm (range 52.2–53.2 ppm), and Sm/Nd ratios ranged from 0.1344 to 0.1372. The analytical data are reported in Table DR3.

### **U-Pb analysis of igneous zircon (SHRIMP: Australian National University)**

U-Pb zircon age determinations were made using SHRIMP II and SHRIMP-RG at the Australian National University Research School of Earth Sciences (ANU-RSES) following the procedures described in Williams (1998 and references therein). Data were reduced using the SQUID Excel Macro (Ludwig, 2001). The zircon U/Pb ratios have been normalized relative to a value of 0.0668 for the Temora reference zircon, equivalent to an age of 417 Ma (Black *et al.* 2003); analytical uncertainties for the respective analytical sessions are given in the footnotes to Table DR4. Uncertainties reported in Table DR4 for individual analyses (ratios and ages) are given at the 1σ level. Tera–Wasserburg (Tera and Wasserburg, 1972) concordia plots, probability density plots with stacked histograms, and weighted mean <sup>238</sup>U/<sup>206</sup>Pb age calculations were calculated using ISOPLOT/EX (Ludwig, 2003). Where appropriate the “Mixture Modelling”

algorithm of Sambridge and Compston (1994) via ISOPLOT/EX has been used to un-mix statistical age populations or groupings. From such groupings weighted mean  $^{238}\text{U}/^{206}\text{Pb}$  ages have been calculated and the uncertainties reported as 95% confidence limits, including incorporation, in quadrature, of the uncertainty in the reference zircon calibration. The analytical data are reported in Table DR4.

#### **U–Pb analyses of zircon (LA-ICP-MS: University of Arizona)**

Zircon grains (generally 500–1000 for sedimentary rocks and 50–100 for igneous rocks) were incorporated into a 1" epoxy mount together with fragments of the Sri Lanka standard zircon at the University of Arizona. The mounts were sanded down to a depth of ~20 microns, polished, imaged, and cleaned prior to isotopic analysis.

U–Pb geochronology of zircons was conducted by laser ablation multicollector inductively coupled plasma mass spectrometry (LA-MC-ICPMS) at the Arizona LaserChron Center (Gehrels et al., 2006, 2008). The analyses involve ablation of zircon with a New Wave DUV193 Excimer laser (operating at a wavelength of 193 nm) using a spot diameter of 35  $\mu\text{m}$ . The ablated material is carried in helium into the plasma source of a GVI Isoprobe, which is equipped with a flight tube of sufficient width that U, Th, and Pb isotopes are measured simultaneously. All measurements are made in static mode, using Faraday detectors with  $10^{11}$  ohm resistors for  $^{238}\text{U}$ ,  $^{232}\text{Th}$ ,  $^{208}\text{Pb}$ , and  $^{206}\text{Pb}$ , a Faraday detector with a  $10\text{e}12$  ohm resistor for  $^{207}\text{Pb}$ , and an ion-counting channel for  $^{204}\text{Pb}$ . Ion yields are ~1.0 mv per ppm. Each analysis consists of one 12-second integration on peaks with the laser off (for backgrounds), 12 one-second integrations with the laser firing, and a 30 second delay to purge the previous sample and prepare for the next analysis. The ablation pit is ~12 microns in depth.

For each analysis, the errors in determining  $^{206}\text{Pb}/^{238}\text{U}$  and  $^{206}\text{Pb}/^{204}\text{Pb}$  result in a measurement error of ~1–2% (at 2-sigma level) in the  $^{206}\text{Pb}/^{238}\text{U}$  age. The errors in measurement of  $^{206}\text{Pb}/^{207}\text{Pb}$  and  $^{206}\text{Pb}/^{204}\text{Pb}$  also result in ~1–2% (at 2-sigma level) uncertainty in age for grains that are >1.0 Ga, but are substantially larger for younger grains due to low intensity of the  $^{207}\text{Pb}$  signal. For most analyses, the cross-over in precision of  $^{206}\text{Pb}/^{238}\text{U}$  and  $^{206}\text{Pb}/^{207}\text{Pb}$  ages occurs at ~1.0 Ga.

Common Pb correction is accomplished by using the measured  $^{204}\text{Pb}$  and assuming an initial Pb composition from Stacey and Kramers (1975) (with uncertainties of 1.0 for  $^{206}\text{Pb}/^{204}\text{Pb}$  and 0.3 for  $^{207}\text{Pb}/^{204}\text{Pb}$ ). Our measurement of  $^{204}\text{Pb}$  is unaffected by the presence of  $^{204}\text{Hg}$  because backgrounds are measured on peaks (thereby subtracting any background  $^{204}\text{Hg}$  and  $^{204}\text{Pb}$ ), and because very little Hg is present in the argon gas (background  $^{204}\text{Hg}$  = ~300 CPS).

Inter-element fractionation of Pb/U is generally ~20%, whereas apparent fractionation of Pb isotopes is generally <1%. In-run analysis of fragments of a large zircon crystal (generally every fifth measurement) with known age of  $563.5 \pm 3.2$  Ma (2-sigma error) is used to correct for this fractionation. The uncertainty resulting from the calibration correction is generally 1–2% (2-sigma) for both  $^{206}\text{Pb}/^{207}\text{Pb}$  and  $^{206}\text{Pb}/^{238}\text{U}$  ages.

Concentrations of U and Th are calibrated relative to our Sri Lanka zircon, which contains ~518 ppm of U and 68 ppm Th.

The analytical data for zircon from igneous rocks are reported in Table DR5 and for detrital zircon in Table DR6. Uncertainties shown in these tables are at the 1-sigma level, and include only measurement errors. Analyses that are >30% discordant (by comparison of  $^{206}\text{Pb}/^{238}\text{U}$  and  $^{206}\text{Pb}/^{207}\text{Pb}$  ages) or >5% reverse discordant are not considered further.

#### **Whole-rock oxygen isotope compositions (University of Wisconsin, Madison)**

Whole-rock powders were analyzed in the University of Wisconsin Stable Isotope Laboratory by laser fluorination following the procedure described in Lackey et al. (2011). Isotope ratios were measured on a dual inlet gas source Finnigan MAT 251 mass spectrometer. Oxygen was extracted from 2–3 mg samples with  $\text{BrF}_5$  using a 30W  $\text{CO}_2$  laser ( $l = 10.6 \text{ mm}$ ), then purified cryogenically, passed through hot Hg to remove any residual  $\text{F}_2$ , and finally converted to  $\text{CO}_2$  with a hot carbon rod (Valley et al., 1995). Analyses were standardized by running five analyses of UWG-2, the Gore Mountain garnet standard;  $\delta^{18}\text{O}$  values were corrected to the long-term accepted value of 5.80‰ for UWG-2. The average raw  $\delta^{18}\text{O}$  of UWG-2 for five analyses is  $5.76 \pm 0.08\text{\textperthousand}$ , one standard deviation. The analytical data are reported in Table DR7.

### **Lu–Hf isotope analyses of detrital zircons (University of Arizona)**

Hf isotope analyses are conducted with a Nu HR ICPMS connected to a Photon Machines Analyte G2 excimer laser at the University of Arizona following the procedure outlined in Cecil et al. (2011). Instrument settings are established first by analysis of 10 ppb solutions of JMC475 and a Spex Hf solution, and then by analysis of 10 ppb solutions containing Spex Hf, Yb, and Lu. The mixtures range in concentration of Yb and Lu, with  $^{176}(\text{Yb+Lu})$  up to 70% of the  $^{176}\text{Hf}$ . When all solutions yield  $^{176}\text{Hf}/^{177}\text{Hf}$  of  $\sim 0.28216$ , instrument settings are optimized for laser ablation analyses and seven different standard zircons (Mud Tank, 91500, Temora, R33, FC52, Plesovice, and Sri Lanka) are analyzed. These standards are included with unknowns on the same epoxy mounts. When precision and accuracy are acceptable, unknowns are analyzed using exactly the same acquisition parameters.

Laser ablation analyses are conducted with a laser beam diameter of 40 microns, with the ablation pits located on top of the U–Pb analysis pits. CL images are used to ensure that the ablation pits do not overlap multiple age domains or inclusions. Each acquisition consists of one 40-second integration on backgrounds (on peaks with no laser firing) followed by 60 one-second integrations with the laser firing. Using a typical laser fluence of  $\sim 5 \text{ J/cm}^2$  and pulse rate of 7 hz, the ablation rate is  $\sim 0.8$  microns per second. Each standard is analyzed once for every  $\sim 20$  unknowns.

Isotope fractionation is accounted for using the method of Woodhead et al. (2004):  $\beta\text{Hf}$  is determined from the measured  $^{179}\text{Hf}/^{177}\text{Hf}$ ,  $\beta\text{Yb}$  is determined from the measured  $^{173}\text{Yb}/^{171}\text{Yb}$  (except for very low Yb signals);  $\beta\text{Lu}$  is assumed to be the same as  $\beta\text{Yb}$ ; and an exponential formula is used for fractionation correction. Yb and Lu interferences are corrected by measurement of  $^{176}\text{Yb}/^{171}\text{Yb}$  and  $^{176}\text{Lu}/^{175}\text{Lu}$  (respectively), as advocated by Woodhead et al. (2004). Critical isotope ratios are  $^{179}\text{Hf}/^{177}\text{Hf} = 0.73250$  (Patchett and Tatsumoto, 1980);  $^{173}\text{Yb}/^{171}\text{Yb} = 1.132338$  (Vervoort et al. 2004);  $^{176}\text{Yb}/^{171}\text{Yb} = 0.901691$  (Vervoort et al., 2004; Amelin and Davis, 2005);  $^{176}\text{Lu}/^{175}\text{Lu} = 0.02653$  (Patchett, 1983). All corrections are done line-by-line. For very low Yb signals,  $\beta\text{Hf}$  is used for fractionation of Yb isotopes. The corrected  $^{176}\text{Hf}/^{177}\text{Hf}$  values are filtered for outliers (2-sigma filter), and the average and standard error are calculated from the resulting  $\sim 58$  integrations. There is no capability to use only a portion of the acquired data.

All solutions, standards, and unknowns analyzed during a session are reduced together. The cutoff for using  $\beta\text{Hf}$  versus  $\beta\text{Yb}$  is determined by monitoring the average offset of the standards from their known values, and the cutoff is set at the minimum offset. For most data sets, this is achieved at  $\sim 6$  mv of  $^{171}\text{Yb}$ . For sessions in which the standards yield  $^{176}\text{Hf}/^{177}\text{Hf}$  values that are shifted consistently from the known values, a correction factor is applied to the

$^{176}\text{Hf}/^{177}\text{Hf}$  of all standards and unknowns. This correction factor, which is not necessary for most sessions, averages 1 epsilon unit.

The  $^{176}\text{Hf}/^{177}\text{Hf}$  at time of crystallization is calculated from measurement of present-day  $^{176}\text{Hf}/^{177}\text{Hf}$  and  $^{176}\text{Lu}/^{177}\text{Hf}$ , using the decay constant of  $^{176}\text{Lu}$  ( $\lambda = 1.867 \times 10^{-11}$ ) from Scherer et al. (2001) and Söderlund et al. (2004). No capability is provided for calculating Hf Depleted Mantle model ages because the  $^{176}\text{Hf}/^{177}\text{Hf}$  and  $^{176}\text{Lu}/^{177}\text{Hf}$  of the source material(s) from which the zircon crystallized is not known. The analytical data are reported in Table DR8.

### Lu–Hf and O analysis of igneous zircon (Australian National University)

Following the U–Pb analyses, the SHRIMP 1–2  $\mu\text{m}$  deep U–Pb pits were lightly polished away and oxygen isotope analyses made in same location using SHRIMP II fitted with a Cs ion source and electron gun for charge compensation as described by Ickert et al. (2008). Oxygen isotope ratios were determined in multiple collector mode using an axial continuous electron multiplier (CEM) triplet collector, and two floating heads with interchangeable CEM–Faraday Cups. The Temora 2 and FC1 reference zircons were analysed to monitor and correct for isotope fractionation. The measured  $^{18}\text{O}/^{16}\text{O}$  ratios and calculated  $\delta^{18}\text{O}$  values have been normalised relative to an FC1 weighted mean  $\delta^{18}\text{O}$  value of +5.4 ‰ (Ickert et al. 2008). Reproducibility in the Duluth Gabbro FC1 reference zircon  $\delta^{18}\text{O}$  value ranged from  $\pm 0.30\text{‰}$  to  $0.44\text{‰}$  ( $2\sigma$  uncertainty) for the analytical sessions. As a secondary reference, the Temora 2 zircon was analysed in the same sessions, which gave  $\delta^{18}\text{O}$  values of +8.2‰ in agreement with data reported by Ickert et al. (2008).

Lu–Hf isotope measurements were conducted by laser ablation multicollector inductively coupled plasma mass spectroscopy (LA–MC–ICPMS) using the ANU-RSES Neptune MC–ICPMS coupled with a 193 nm ArF Excimer laser, following procedures similar to those described in Munizaga et al. (2008). For all analyses of unknowns or secondary standards, the laser spot size was ~47  $\mu\text{m}$  in diameter. Laser ablation analyses targeted the same locations within single zircon grains used for both the U–Pb and oxygen isotope analyses described above. The mass spectrometer was first tuned to optimal sensitivity using a large grain of zircon from the Mud Tank carbonatite. Isotopic masses were measured simultaneously in static-collection mode. A gas blank was acquired at regular intervals throughout the analytical session (every 12 analyses). Typically the laser was fired with a 5–8 Hz repetition rate and 50–60 mJ energy. Data were acquired for 100 seconds, but in many cases only a selected interval from the total acquisition was used in data reduction.

Throughout the analytical session several widely used reference zircons (FC-1 and Temora 2) were analysed to monitor data quality and reproducibility. Signal intensity was typically ~5–6 V for total Hf at the beginning of ablation, and decreased over the acquisition time to 2 V or less. Isobaric interferences of  $^{176}\text{Lu}$  and  $^{176}\text{Yb}$  on the  $^{176}\text{Hf}$  signal were corrected by monitoring signal intensities of  $^{175}\text{Lu}$  and  $^{173}\text{Yb}$ ,  $^{172}\text{Yb}$  and  $^{171}\text{Yb}$ . The calculation of signal intensity for  $^{176}\text{Hf}$  also involved independent mass bias corrections for Lu and Yb (see Munizaga et al. 2008 for further details). During the course of this data collection the reference zircons gave the following weighted mean  $^{176}\text{Hf}/^{177}\text{Hf}$  ratios:  $915000 = 0.282310 \pm 14$  ( $\pm 2\sigma$ ) for 23 analyses, Mud Tank =  $0.282516 \pm 11$  for 8 analyses, FC1 =  $0.282173 \pm 9$  for 22 of 23 analyses, Plesovice =  $0.282486 \pm 11$  for 16 of 17 analyses, and Monastery =  $0.282744 \pm 12$  for 8 analyses. These are within analytical uncertainty of the values reported by Woodhead and Herdt (2005). The analytical data are reported in Table DR9.

## REFERENCES

- Amelin, Y., and Davis, W. J., 2005, Geochemical test for branching decay of  $^{176}\text{Lu}$ : *Geochimica et Cosmochimica Acta*, v. 69, p. 465-473.  
doi:<http://dx.doi.org/10.1016/j.gca.2004.04.028>.
- Black, L. P., Kamo, S. L., Allen, C. M., Aleinikoff, J. N., Davis, D. W., Korsch, R. J., and Foudoulis, C., 2003, TEMORA 1: a new zircon standard for Phanerozoic U-Pb geochronology: *Chemical geology*, v. 200, p. 155-170.  
doi:[http://dx.doi.org/10.1016/S0009-2541\(03\)00165-7](http://dx.doi.org/10.1016/S0009-2541(03)00165-7).
- Boyd, F. R., and Mertzman, S. A., 1987, Composition and structure of the Kaapvaal lithosphere, southern Africa, in Mysen, B. O., ed., *Magmatic Processes: Physiochemical Principles.*, Volume 1, p. 13-24.
- Cecil, M. R., Gehrels, G. E., Ducea, M. N., and Patchett, P. J., 2011, U-Pb-Hf characterization of the central Coast Mountains Batholith; implications for petrogenesis and crustal architecture: *Lithosphere*, v. 3, p. 247-260. doi:[10.1130/1134.1](https://doi.org/10.1130/1134.1).
- Gehrels, G., Valencia, V., and Pullen, A., 2006, Detrital zircon geochronology by laser-ablation multicollector ICPMS at the Arizona Laserchron Center: *Paleontological Society Papers*, v. 12, p. 67.
- Gehrels, G. E., Valencia, V. A., and Ruiz, J., 2008, Enhanced precision, accuracy, efficiency, and spatial resolution of U-Pb ages by laser ablation–multicollector–inductively coupled plasma–mass spectrometry: *Geochemistry, Geophysics, Geosystems*, v. 9, p. Q03017.  
doi:[10.1029/2007gc001805](https://doi.org/10.1029/2007gc001805).
- Ickert, R. B., Hiess, J., Williams, I. S., Holden, P., Ireland, T. R., Lanc, P., Schram, N., Foster, J. J., and Clement, S. W., 2008, Determining high precision, in situ, oxygen isotope ratios with a SHRIMP II: Analyses of MPI-DING silicate-glass reference materials and zircon from contrasting granites: *Chemical geology*, v. 257, p. 114–128.  
doi:<http://dx.doi.org/10.1016/j.chemgeo.2008.08.024>.
- Korhonen, F. J., Saito, S., Brown, M., Siddoway, C. S., and Day, J. M. D., 2010, Multiple Generations of Granite in the Fosdick Mountains, Marie Byrd Land, West Antarctica: Implications for Polyphase Intracrustal Differentiation in a Continental Margin Setting: *Journal of Petrology*, v. 51, p. 627–670. doi:[10.1093/petrology/egp093](https://doi.org/10.1093/petrology/egp093).
- Lackey, J. S., Erdmann, S., Hark, J. S., Nowak, R. M., Murray, K. E., Clarke, D. B., and Valley, J. W., 2011, Tracing garnet origins in granitoid rocks by oxygen isotope analysis: Examples from the South Mountain Batholith, Nova Scotia: *The Canadian Mineralogist*, v. 49, p. 417–439. doi:[10.3749/canmin.49.2.417](https://doi.org/10.3749/canmin.49.2.417).
- Ludwig, K. R., 2003, User's manual for ISOPLOT 3, A Geochronological Toolkt for Microsoft Excel: Berkeley Geochronology Center, Special Publication No. 4.
- Ludwig, K. R., 2001, User's guide to SQUID 2.2: Berkeley, Berkeley Geochronology Center.
- Munizaga, F., Maksaev, V., Fanning, C. M., Giglio, S., Yaxley, G., and Tassinari, C. C. G., 2008, Late Paleozoic, Early Triassic magmatism on the western margin of Gondwana: Collahuasi area, Northern Chile: *Gondwana Research*, v. 13, p. 407–427.  
doi:<http://dx.doi.org/10.1016/j.gr.2007.12.005>.
- Patchett, P. J., 1983, Importance of the Lu-Hf isotopic system in studies of planetary chronology and chemical evolution: *Geochimica et Cosmochimica Acta*, v. 47, p. 81-91.  
doi:[http://dx.doi.org/10.1016/0016-7037\(83\)90092-3](http://dx.doi.org/10.1016/0016-7037(83)90092-3).

- Patchett, P. J., and Tatsumoto, M., 1980, Hafnium isotope variations in oceanic basalts: *Geophysical Research Letters*, v. 7, p. 1077–1080. doi:10.1029/GL007i012p01077.
- Sambridge, M. S., and Compston, W., 1994, Mixture modeling of multi-component data sets with application to ion-probe zircon ages: *Earth and Planetary Science Letters*, v. 128, p. 373–390. doi:10.1016/0012-821x(94)90157-0.
- Scherer, E., Münker, C., and Mezger, K., 2001, Calibration of the Lutetium-Hafnium Clock: *Science*, v. 293, p. 683–687. doi:10.1126/science.1061372.
- Söderlund, U., Patchett, J. P., Vervoort, J. D., and Isachsen, C. E., 2004, The Lu-176 decay constant determined by Lu-Hf and U-Pb isotope systematics of Precambrian mafic intrusions: *Earth and Planetary Science Letters*, v. 219, p. 311–324. doi:10.1016/S0012-821X(04)00012-3.
- Stacey, J. S., and Kramers, J. D., 1975, Approximation of terrestrial lead isotope evolution by a two-stage model: *Earth and Planetary Science Letters*, v. 26, p. 207–221. doi:[http://dx.doi.org/10.1016/0012-821X\(75\)90088-6](http://dx.doi.org/10.1016/0012-821X(75)90088-6).
- Tera, F., and Wasserburg, G. J., 1972, U-Th-Pb systematics in three Apollo 14 basalts and the problem of initial Pb in lunar rocks: *Earth and Planetary Science Letters*, v. 14, p. 281–304. doi:10.1016/0012-821x(72)90128-8.
- Valley, J. W., Kitchen, N., Kohn, M. J., Niendorf, C. R., and Spicuzza, M. J., 1995, UWG-2, a garnet standard for oxygen isotope ratios; strategies for high precision and accuracy with laser heating: *Geochimica et Cosmochimica Acta*, v. 59, p. 5223–5231.
- Vervoort, J. D., Patchett, P. J., Söderlund, U., and Baker, M., 2004, Isotopic composition of Yb and the determination of Lu concentrations and Lu/Hf ratios by isotope dilution using MC-ICPMS: *Geochemistry, Geophysics, Geosystems*, v. 5, p. Q11002. doi:10.1029/2004gc000721.
- Williams, I. S., 1998, U-Th-Pb geochronology by ion microprobe, Socorro, New Mexico, *Reviews in Economic Geology*, Society of Economic Geologists, Applications of microanalytical techniques to understanding mineralizing processes, p. 1–35.
- Woodhead, J., Hergt, J., Shelley, M., Eggin, S., and Kemp, R., 2004, Zircon Hf-isotope analysis with an excimer laser, depth profiling, ablation of complex geometries, and concomitant age estimation: *Chemical Geology*, v. 209, p. 121–135.

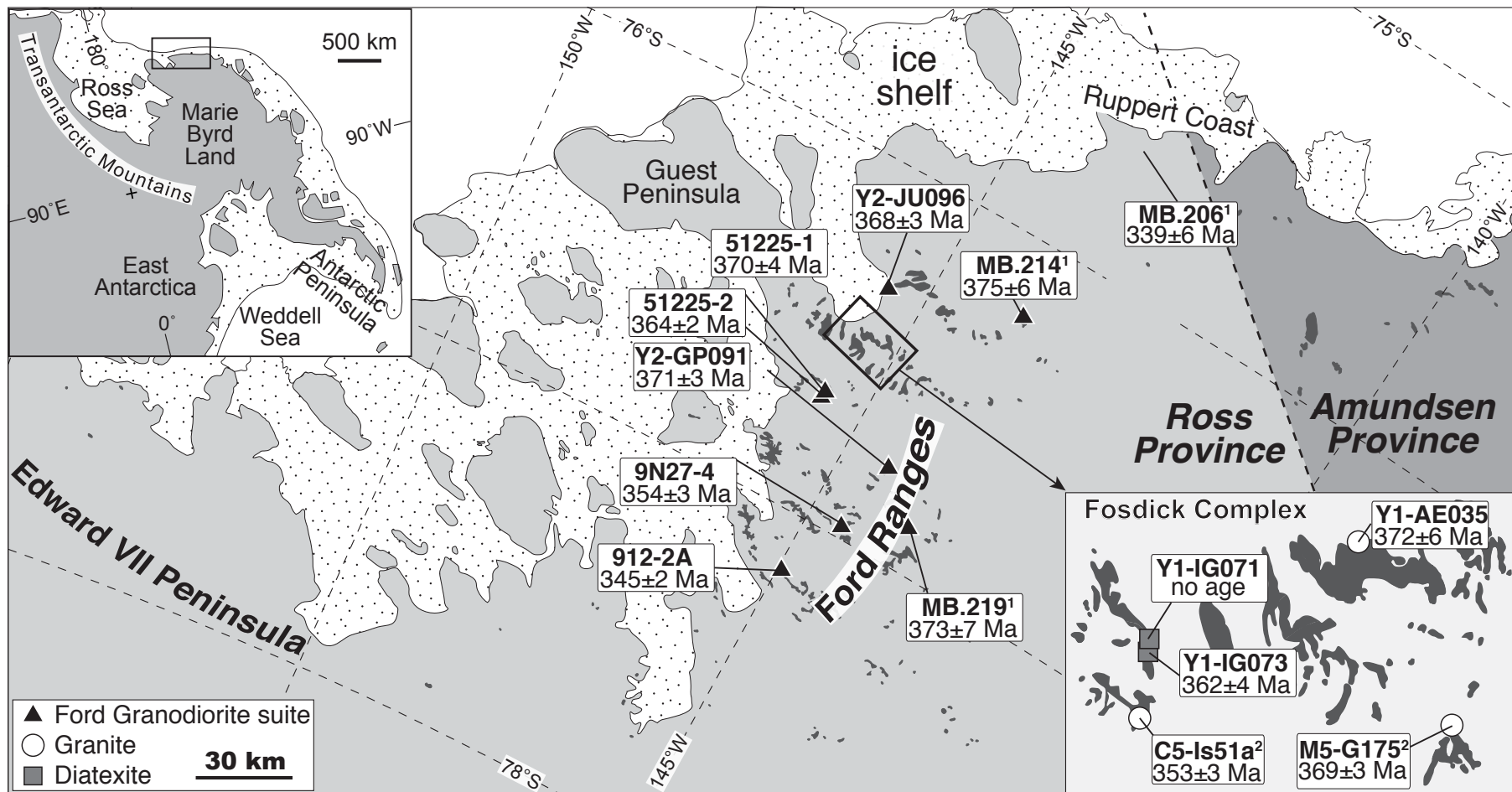


**Figure DR1.** Ages of the Ford Granodiorite suite as well as Devonian–Carboniferous granites and diatexites from the Fosdick complex. Ages are from this study in addition to: <sup>1</sup>Pankhurst et al. (1998); <sup>2</sup>Siddoway and Fanning (2009).

**Table DR1. Sample Locations**

Sample	Rock Type	Location	Latitude	Longitude
10CY-001	Swanson Formation	Clark Mountains	77°16.729' S	142°09.726' W
10CY-002	Swanson Formation	Clark Mountains	77°16.729' S	142°09.726' W
Y2-BR086	Swanson Formation	Bailey Ridge	77°09.679' S	145°16.739' W
Y2-MD092	Swanson Formation	Mount Dolber	77°04.219' S	145°45.077' W
Y2-MP098	Swanson Formation	Mount Passel	76°53.851' S	144°52.003' W
318-M9	Metasedimentary gneiss	Mitchell Peak	76°25.000' S	147°22.000' W
21223-3	Metasedimentary gneiss	Scott Nunataks	77°14.000' S	154°12.000' W
21223-8	Metasedimentary gneiss	Scott Nunataks	77°14.000' S	154°12.000' W
8D27-10	Metasedimentary gneiss	Mt Woodward	77°18.000' S	145°47.000' W
912-2A	Ford Granodiorite Suite	Asman Ridge	77°10.000' S	144°48.000' W
9N27-4	Ford Granodiorite Suite	Mount Ralph	76°58.000' S	144°32.000' W
51225-1	Ford Granodiorite Suite	Chester Mountains	76°40.000' S	145°35.000' W
51225-2	Ford Granodiorite Suite	Chester Mountains	76°40.000' S	145°35.000' W
Y2-GP091	Ford Granodiorite Suite	Greer Peak	76°46.570' S	144°25.644' W
Y2-HN097	Ford Granodiorite Suite	Herman Nunatak	76°13.377' S	143°52.879' W
Y2-JU096	Ford Granodiorite Suite	Mount June	76°15.109' S	145°16.515' W
Y2-SM095	Ford Granodiorite Suite	Saunders Mountain	76°51.104' S	145°41.644' W
Y1-AE035	Devonian–Carboniferous Granite	Mount Avers	76°27.950' S	145°16.324' W
M5-G175	Devonian–Carboniferous Granite	Mount Getz	76°33.180' S	145°13.200' W
Y1-IG071	Diatexite	Mount Iphigene	76°30.676' S	145°48.368' W
Y1-IG073	Diatexite	Mount Iphigene	76°30.676' S	145°48.368' W

**Table DR2. Major element, trace element and REE concentrations**

Rock Type	Swanson Formation					Ford Granodiorite Suite					
	Sample no.	10CY-001	10CY-002	Y2-BR086	Y2-MD092	Y2-MP098	51225-1	51225-2	Y2-GP091	Y2-HN097	Y2-JU096
<i>wt %</i>											
SiO <sub>2</sub>	64.33	63.92	71.59	73.92	74.06	68.24	66.43	67.50	69.08	69.10	67.38
TiO <sub>2</sub>	0.68	0.70	0.73	0.57	0.68	0.70	0.78	0.59	0.53	0.54	0.68
Al <sub>2</sub> O <sub>3</sub>	15.86	16.52	14.02	11.54	12.00	15.13	15.37	15.35	14.98	15.00	15.29
Fe <sub>2</sub> O <sub>3</sub>	0.70	0.74	0.58	0.21	0.57	0.39	0.56	0.89	0.83	0.53	1.06
FeO	5.70	5.82	4.08	4.03	4.06	3.61	4.01	2.47	2.43	2.68	3.14
MnO	0.11	0.11	0.08	0.11	0.11	0.07	0.07	0.06	0.06	0.05	0.07
MgO	3.69	3.76	2.41	2.97	2.78	1.42	1.62	2.02	1.77	1.66	2.35
CaO	3.01	1.25	0.94	2.31	1.47	2.67	2.59	3.20	3.15	2.74	3.92
Na <sub>2</sub> O	2.20	2.44	1.70	1.57	1.93	3.19	3.03	3.83	3.97	3.48	3.40
K <sub>2</sub> O	3.02	4.24	3.36	2.33	2.15	3.70	4.19	3.05	2.52	3.35	2.63
P <sub>2</sub> O <sub>5</sub>	0.18	0.17	0.19	0.17	0.18	0.22	0.24	0.18	0.17	0.16	0.17
LOI	1.50	1.86	2.05	0.98	1.97	1.06	1.05	1.62	0.94	1.71	1.36
Total	100.11	100.32	100.13	100.18	100.44	99.74	99.34	99.42	99.76	99.59	100.44
<i>ppm (XRF)</i>											
Rb	140	195.9	162.8	98.9	95.9	189.2	208.7	143.8	88.1	116.9	98.5
Sr	207	149	137	196	155	223	218	378	354	418	346
Y	32	33.6	39.4	33.4	38.8	32.4	34.8	23	23.7	35.2	27
Zr	123	121	172	166	233	228	240	146	143	173	155
V	131	112	89	80	84	73	82	77	72	73	97
Ni	110	118	43	106	112	9	10	37	35	34	35
Cr	110	118	84	123	151	33	36	60	80	64	78
Nb	11.6	13.4	15.2	11.7	13.5	19.7	21.3	13.2	15.1	14.5	10.1
Ga	20.6	21.2	18.9	15.7	17.1	21.5	21.7	18.7	19.5	19.2	19
Cu	39	41	6	8	30	12	23	9	9	9	9
Zn	120	152	85	74	78	66	73	48	46	53	59
Co	26	28	18	17	17	11	14	12	11	11	15
Ba	483	658	727	426	438	514	565	483	472	628	525
La	26	29	32	30	37	34	44	24	23	38	29
Ce	69	75	82	65	83	75	105	51	44	80	55
U	3.1	1.4	3.8	1.9	3.8	5.1	5.3	2.1	4.9	4.7	2.3
Th	14.2	17.2	14.3	13.7	13.3	14.8	24.5	14.5	5.4	16.2	9.4
Sc	18	16	12	12	12	11	12	11	9	11	11
Pb	8	12	15	11	3	15	28	<1	10	189	22
<i>ppm (ICP-MS)</i>											
Sc	18.2	17.31	11.19	9.8	10.44	10.92	11.28	8.64	8.72	9.59	11.42
Y	28.59	30.36	38.89	27.05	31.32	34.49	33.81	20.93	19	30.66	22.45
La	32.26	37.35	42.9	32.66	36.72	47.96	53.18	25.03	21.02	40.53	22.35
Ce	66.58	76.4	90.12	66.73	75.01	103.16	114.31	50.07	41.61	82.65	48.97
Pr	7.83	8.84	10.6	7.92	8.97	12.8	14.07	6.16	5.04	10.03	6.05
Nd	30.03	34.16	40.27	30.29	34.16	48.3	52.72	23.34	19.32	37.43	23.07
Sm	6.25	6.96	8.43	6.1	6.92	8.97	9.47	4.65	3.93	6.91	4.63
Eu	1.34	1.44	1.65	1.18	1.29	1.38	1.34	1.06	0.94	1.39	1.16
Gd	5.05	5.52	6.95	4.89	5.47	7.53	7.59	4.21	3.65	6.02	4.3
Tb	0.85	0.91	1.2	0.81	0.93	1.17	1.18	0.69	0.61	0.97	0.7
Dy	5.03	5.26	7.03	4.75	5.5	6.31	6.48	3.9	3.45	5.34	3.94
Ho	1.03	1.07	1.41	0.96	1.14	1.19	1.22	0.74	0.67	1.03	0.77
Er	2.89	3.01	3.83	2.65	3.17	3.51	3.63	2.21	1.99	3.06	2.27
Tm	0.43	0.43	0.55	0.39	0.47	0.55	0.58	0.36	0.32	0.49	0.36
Yb	2.81	2.86	3.45	2.43	3.03	3.39	3.59	2.38	2.03	3.09	2.29
Lu	0.39	0.4	0.45	0.33	0.42	0.52	0.56	0.39	0.32	0.49	0.37

**Table DR2.** I

Rock Type Sample no.	Diatexite		Devonian-Carboniferous S	
	Y1-IG071	Y1-IG073	Y1-AE035	M5-G175
<i>wt %</i>				
SiO <sub>2</sub>	72.88	71.63	66.59	67.54
TiO <sub>2</sub>	0.46	0.48	0.87	0.70
Al <sub>2</sub> O <sub>3</sub>	13.91	14.62	16.04	15.23
Fe <sub>2</sub> O <sub>3</sub>	0.49	0.26	1.15	0.92
FeO	2.51	2.39	3.71	3.76
MnO	0.04	0.02	0.06	0.06
MgO	1.36	1.04	1.63	1.96
CaO	1.63	2.08	3.52	1.72
Na <sub>2</sub> O	2.72	2.96	3.68	3.11
K <sub>2</sub> O	4.16	4.00	2.26	4.14
P <sub>2</sub> O <sub>5</sub>	0.08	0.17	0.27	0.09
LOI	1.06	0.98	1.05	1.10
Total	100.52	99.92	100.19	99.65
<i>ppm (XRF)</i>				
Rb	173	150.7	146.4	201
Sr	191	259	281	249
Y	26.1	22.4	23	39.1
Zr	169	255	256	233
V	57	51	100	85
Ni	15	10	10	23
Cr	75	34	58	77
Nb	13.5	11.7	16.6	19.2
Ga	19.1	18.5	22	22.1
Cu	7	7	8	23
Zn	58	50	80	81
Co	8	6	14	15
Ba	551	1109	690	1119
La	24	40	23	36
Ce	53	100	50	87
U	3.7	3.6	2.2	6.2
Th	12.2	22.4	5.7	16.8
Sc	8	8	16	12
Pb	28	33	21	27
<i>ppm (ICP-MS)</i>				
Sc	10.32	7.97	15.77	13.95
Y	17.74	22.49	25.8	35.88
La	31.52	63.83	43.65	58.01
Ce	65.68	131.69	91.8	115.07
Pr	8.16	16	11.32	13.67
Nd	29.77	60.97	44.48	50.09
Sm	6.04	11.12	8.37	8.94
Eu	1.18	1.74	1.76	1.53
Gd	4.92	8.65	6.83	7.82
Tb	0.79	1.24	1.05	1.19
Dy	3.88	5.83	5.38	6.25
Ho	0.64	0.87	0.95	1.19
Er	1.56	1.91	2.54	3.5
Tm	0.2	0.21	0.37	0.53
Yb	1.1	0.96	2.19	3.1
Lu	0.15	0.12	0.33	0.48

**Table DR3. Sr-Nd isotope compositions**

Rock Type Sample no.	Swanson Formation					Ford Granodiorite suite						Carboniferous granite			Diatexites	
	10CY-001	10CY-002	Y2-BR086	Y2-MD092	Y2-MP098	51225-1	51225-2	Y2-GP091	Y2-HN097	Y2-JU096	Y2-SM095	Y1-AE035	M5-G175	Y1-IG071	Y2-IG073	
Rb	131.3	205.5	155.2	99.9	95.5	194.2	220.7	142.5	85.3	122.2	100.4	128.6	213.8	171.17	146.55	
Sr	201.1	147.6	128.7	194.8	150.7	223	220.4	375.9	357.2	422.8	345.6	271.1	248.5	190.47	279.69	
Rb/Sr	0.65	1.39	1.21	0.51	0.63	0.87	1.00	0.38	0.24	0.29	0.29	0.47	0.86	0.90	0.52	
$^{87}\text{Rb}/^{86}\text{Sr}$	2.09	4.04	3.50	1.49	1.84	2.29	2.90	1.10	0.69	0.84	0.84	1.37	2.49	2.60	1.64	
$^{87}\text{Sr}/^{86}\text{Sr}$	0.726291	0.732242	0.738139	0.727782	0.72801	0.720773	0.72163	0.71077	0.708715	0.71085	0.710204	0.715979	0.720081	0.7176359	0.7176359	
$^{87}\text{Sr}/^{86}\text{Sr}_{(100\text{Ma})}$	0.723375	0.726599	0.733244	0.725704	0.725442	0.717575	0.717575	0.709237	0.707749	0.709681	0.709028	0.714059	0.716597	0.7139972	0.7153412	
$^{87}\text{Sr}/^{86}\text{Sr}_{(360\text{Ma})}$	0.715775	0.71189	0.720484	0.720285	0.718746	0.709237	0.707005	0.705241	0.705231	0.706634	0.705965	0.709056	0.707518	0.7045129	0.7093598	
Sm	6.6	6.7	8	6	6.9	9.2	11.2	4.3	3.8	8.6	4.8	6.1	10.2	8.5	11.5	
Nd	35.3	32.8	38.8	30.3	34.3	45.9	59.6	21.5	18.2	46.6	23	31.4	53.6	41.3	61.6	
Sm/Nd	0.19	0.2	0.21	0.2	0.2	0.2	0.19	0.2	0.21	0.18	0.21	0.19	0.19	0.2	0.2	
$^{147}\text{Sm}/^{144}\text{Nd}$	0.113254	0.122727	0.124266	0.120037	0.120772	0.090416	0.113363	0.121087	0.110934	0.126897	0.127007	0.116782	0.114473	0.123871	0.1125472	
$^{143}\text{Nd}/^{144}\text{Nd}$	0.512117	0.512084	0.512079	0.511979	0.512061	0.512378	0.512292	0.512432	0.512276	0.512438	0.512368	0.512254	0.512225	0.5121746	0.512217	
$\epsilon\text{Nd}_{(0\text{Ma})}$	-10.2	-10.8	-10.9	-12.8	-11.3	-5.1	-6.7	-4	-7.1	-3.9	-5.3	-7.5	-8.1	-9.0	-8.2	
$\epsilon\text{Nd}_{(100\text{Ma})}$	-9.1	-9.9	-10	-11.9	-10.3	-3.7	-5.7	-3.1	-6	-3.0	-4.4	-6.5	-7.0	-8.1	-7.1	
$\epsilon\text{Nd}_{(360\text{Ma})}$	-6.3	-7.4	-7.6	-9.3	-7.8	-0.2	-2.9	-0.5	-3.1	-0.7	-2.1	-3.8	-4.3	-5.7	-4.3	

Notes:  $\lambda_{\text{Rb}} = 1.3968 \times 10^{-11}$  $\lambda_{\text{Sm}} = 6.54 \times 10^{-12}$  $^{143}\text{Nd}/^{144}\text{Nd}_{\text{CHUR}(0)} = 0.512638$  $^{147}\text{Sm}/^{144}\text{Nd}_{\text{CHUR}(0)} = 0.1967$









**Table DR5. Summary of LA-ICP-MSP U-Pb results for zircon**

	Spot Size ( $\mu\text{m}$ )	U (ppm)	Th (ppm)	U/Th	Radiogenic Ratios				Age (Ma)			
					$^{206}\text{Pb}/^{238}\text{U}$	2 $\sigma$	$^{207}\text{Pb}/^{235}\text{U}$	2 $\sigma$	$^{206}/^{207}\text{Pb}$	2 $\sigma$	$^{206}\text{Pb}/^{238}\text{U}$	2 $\sigma$
<b>Y1-AE035 – Devonian-Carboniferous granite</b>												
Y1-AE035_16	30	114	52	2.2	0.0537	0.0030	0.4022	0.093	337.2	62.3	337.2	18.4
Y1-AE035_1	30	180	93	1.9	0.0623	0.0018	0.4659	0.049	389.3	42.6	389.3	11.0
Y1-AE035_2	30	261	172	1.5	0.0567	0.0020	0.4182	0.026	355.8	43.1	355.8	12.2
Y1-AE035_3	30	258	119	2.2	0.0578	0.0035	0.4223	0.035	362.4	76.2	362.4	21.0
Y1-AE035_3	30	242	114	2.1	0.0588	0.0009	0.4397	0.036	368.3	20.3	368.3	5.6
Y1-AE035_5	30	207	167	1.2	0.0585	0.0013	0.4453	0.025	366.4	28.1	366.4	7.6
Y1-AE035_6	30	251	84	3	0.0572	0.0021	0.4187	0.039	358.6	46.0	358.6	12.8
Y1-AE035_7	30	472	481	1	0.0598	0.0012	0.4414	0.014	374.5	27.9	374.5	7.4
Y1-AE035_8	30	135	56	2.4	0.0599	0.0025	0.4365	0.046	374.7	57.3	374.7	15.2
Y1-AE035_9	30	310	115	2.7	0.0597	0.0022	0.4427	0.032	374.0	49.7	374.0	13.2
Y1-AE035_9	30	385	200	1.9	0.0583	0.0030	0.4402	0.033	365.1	66.3	365.1	18.2
Y1-AE035_11	30	368	99	3.7	0.0592	0.0027	0.4372	0.026	370.5	60.0	370.5	16.2
Y1-AE035_12	30	259	105	2.5	0.0613	0.0016	0.4546	0.026	383.5	37.4	383.5	9.8
Y1-AE035_13	30	149	60	2.5	0.0605	0.0031	0.4456	0.032	378.8	70.8	378.8	18.6
Y1-AE035_14	30	138	61	2.3	0.0575	0.0018	0.4334	0.046	360.6	40.2	360.6	11.2
Y1-AE035_17	30	145	63	2.3	0.0601	0.0016	0.4342	0.045	376.0	37.6	376.0	10.0
Y1-AE035_18	30	206	127	1.6	0.0593	0.0015	0.4441	0.032	371.4	34.4	371.4	9.2
Y1-AE035_19	30	137	62	2.2	0.0583	0.0020	0.4276	0.046	365.1	43.8	365.1	12.0
Y1-AE035_20	30	140	53	2.7	0.0606	0.0037	0.4395	0.062	379.4	84.9	379.4	22.4
Y1-AE035_21	30	227	107	2.1	0.0609	0.0009	0.4469	0.023	381.1	21.7	381.1	5.6
Y1-AE035_22	30	106	44	2.4	0.0584	0.0021	0.4411	0.063	365.9	46.4	365.9	12.6
Y1-AE035_23	30	240	101	2.4	0.0608	0.0020	0.4415	0.036	380.2	47.3	380.2	12.4
Y1-AE035_24	30	138	64	2.1	0.0598	0.0019	0.4446	0.064	374.2	43.3	374.2	11.6
Y1-AE035_25	30	207	168	1.2	0.0586	0.0017	0.4294	0.035	367.1	37.9	367.1	10.4

\*1.3=Systematic error of  $^{206}\text{Pb}/^{238}\text{U}$  age based on Sri Lankan standard

Notes:

- <sup>1</sup> Analyses with >10% uncertainty (1-sigma) in 206Pb/238U age are not included.
- <sup>2</sup> Analyses with >10% uncertainty (1-sigma) in 206Pb/207Pb age are not included, unless 206Pb/238U age is <500 Ma.
- <sup>3</sup> Best age is determined from 206Pb/238U age for analyses with 206Pb/238U age <1000 Ma and from 206Pb/207Pb age for analyses with 206Pb/238U age > 1000 Ma.
- <sup>4</sup> Concordance is based on 206Pb/238U age / 206Pb/207Pb age. Value is not reported for 206Pb/238U ages <500 Ma because of large uncertainty in 206Pb/238U age.
- <sup>5</sup> Analyses with 206Pb/238U age > 500 Ma and with >20% discordance (<80% concordance) are not included.
- <sup>6</sup> Analyses with 206Pb/238U age > 500 Ma and with >5% reverse discordance (<105% concordance) are not included.
- <sup>7</sup> Analyses conducted by LA-MC-ICPMS, as described by Gehrels et al. (2008).
- <sup>8</sup> U concentration and U/Th are calibrated relative to Sri Lanka zircon standard and are accurate to ~20%.
- <sup>9</sup> Common Pb correction is from measured 204Pb with common Pb composition interpreted from Stacey and Kramers (1975).
- <sup>10</sup> Common Pb composition assigned uncertainties of 1.5 for 206Pb/204Pb, 0.3 for 207Pb/204Pb, and 2.0 for 208Pb/204Pb.
- <sup>11</sup> U/Pb and 206Pb/207Pb fractionation is calibrated relative to fragments of a large Sri Lanka zircon of  $563.5 \pm 3.2$  Ma (2-sigma).
- <sup>12</sup> U decay constants and composition as follows:  $^{238}\text{U} = 9.8485 \times 10^{-10}$ ,  $^{235}\text{U} = 1.55125 \times 10^{-10}$ ,  $^{238}\text{U}/^{235}\text{U} = 137.88$ .











**Table DR7. Whole-rock oxygen isotope results**

Sample	Std/Unkn	mg	$\mu\text{ml}$	$\mu\text{ml}/\text{mg}$	$\delta^{18}\text{O}$ raw	$\delta^{18}\text{O}$ crrtd (smow)
UWG-2	std	2.50	32.1	12.8	5.68	
UWG-2	std	2.95	38.4	13.0	5.66	
UWG-2	std	3.36	41.3	12.3	5.83	
UWG-2	std	4.00	51.2	12.8	5.80	
K6-SR29a	WR	2.53	36.3	14.3	12.73	12.77
K6-SR30	WR	2.58	38.2	14.8	13.44	13.48
K6-SR32	WR	3.09	45.4	14.7	9.96	10.00
10CY-001	WR	2.41	35.4	14.7	-6.89	-6.85
10CY-002	WR	2.74	39.7	14.5	-9.16	-9.12
Y2-MP098	WR	2.77	40.4	14.6	11.98	12.02
Y2-BR086	WR	2.44	35.9	14.7	10.00	10.04
Y2-MD092	WR	2.97	42.3	14.2	13.29	13.33
UWG-2	std	3.06	39.7	13.0	5.81	

Notes:

UWG-2: n= 5, x = 5.76,  $\pm$  0.08, 1 St. Dev.

**Table DR8. Hf isotope analyses for detrital zircons**

Spot	Age (Ma)	( $^{176}\text{Yb} + ^{176}\text{Lu}$ ) / $^{176}\text{Hf}$ (%)	Volts Hf	$^{176}\text{Hf}/^{177}\text{Hf}$	$\pm$ (1s)	$^{176}\text{Lu}/^{177}\text{Hf}$	$^{176}\text{Hf}/^{177}\text{Hf}_{(t)}$	$\epsilon_{\text{Hf}(0)}$	$\pm$ 1s	$\epsilon_{\text{Hf}(t)}$
<b>Y2-MP098</b>										
6	595	9.3	2.5	0.281726	0.000031	0.000689	0.281719	-37.4	1.1	-24.5
9	541	6.9	2.2	0.282313	0.000031	0.000407	0.282309	-16.7	1.1	-4.8
10	1819	17.6	2.3	0.281711	0.000041	0.001156	0.281671	-38.0	1.5	1.7
12	1117	18.4	2.2	0.282223	0.000030	0.001230	0.282197	-19.9	1.0	4.3
13	1168	57.6	1.5	0.282246	0.000048	0.003033	0.282179	-19.1	1.7	4.8
14	2782	13.4	1.9	0.280949	0.000030	0.000802	0.280906	-64.9	1.1	-3.1
16	1023	14.3	2.7	0.282312	0.000028	0.000787	0.282297	-16.7	1.0	5.7
17	947	17.9	1.7	0.282286	0.000041	0.001110	0.282266	-17.7	1.5	2.8
19	770	28.2	2.3	0.282312	0.000036	0.001681	0.282288	-16.7	1.3	-0.4
21	1054	8.1	2.2	0.282380	0.000038	0.000499	0.282370	-14.3	1.3	9.0
22	551	2.8	2.3	0.282295	0.000029	0.000167	0.282293	-17.3	1.0	-5.1
27	1046	11.6	2.1	0.282226	0.000028	0.000703	0.282212	-19.8	1.0	3.2
33	508	36.5	2.5	0.282236	0.000038	0.002256	0.282214	-19.4	1.4	-8.9
35	982	36.2	1.7	0.282273	0.000044	0.002210	0.282232	-18.1	1.6	2.4
40	998	9.3	1.6	0.282116	0.000037	0.000607	0.282105	-23.7	1.3	-1.7
43	589	2.2	2.1	0.282439	0.000029	0.000129	0.282437	-12.3	1.0	0.8
46	567	11.9	2.2	0.282375	0.000029	0.000714	0.282367	-14.5	1.0	-2.1
47	568	10.1	2.3	0.282281	0.000037	0.000601	0.282275	-17.8	1.3	-5.4
48	955	25.7	2.1	0.282187	0.000040	0.001441	0.282161	-21.2	1.4	-0.7
49	1868	9.7	2.3	0.281521	0.000031	0.000578	0.281500	-44.7	1.1	-3.3
50	525	5.4	2.1	0.282329	0.000044	0.000326	0.282326	-16.1	1.6	-4.5
53	1068	10.4	2.1	0.282209	0.000033	0.000613	0.282196	-20.4	1.2	3.1
54	1062	10.2	2.0	0.281984	0.000039	0.000611	0.281972	-28.3	1.4	-5.0
58	1731	17.3	2.0	0.281510	0.000038	0.001024	0.281476	-45.1	1.4	-7.3
61	797	12.5	2.2	0.282290	0.000031	0.000853	0.282277	-17.5	1.1	-0.2
62	613	30.6	2.6	0.282071	0.000034	0.001822	0.282050	-25.2	1.2	-12.3
64	1166	4.3	2.3	0.281896	0.000030	0.000212	0.281891	-31.4	1.1	-5.5
65	1090	18.0	2.0	0.282139	0.000035	0.001041	0.282118	-22.8	1.2	0.9
67	1704	15.4	2.0	0.281249	0.000039	0.000946	0.281218	-54.3	1.4	-17.1
70	965	34.5	2.3	0.282129	0.000035	0.001954	0.282093	-23.2	1.2	-2.9
71	686	19.1	1.8	0.282342	0.000038	0.001147	0.282328	-15.6	1.3	-0.9
72	1679	9.6	2.4	0.281849	0.000033	0.000555	0.281831	-33.1	1.2	4.1
75	644	8.0	2.6	0.282446	0.000036	0.000459	0.282440	-12.0	1.3	2.2
76	570	0.9	2.8	0.282492	0.000027	0.000052	0.282491	-10.4	1.0	2.3
78	1749	12.8	2.5	0.281583	0.000033	0.000733	0.281559	-42.5	1.2	-3.9
80	1081	17.0	2.2	0.282401	0.000036	0.001386	0.282372	-13.6	1.3	9.7
82	550	8.5	2.8	0.282295	0.000031	0.000475	0.282291	-17.3	1.1	-5.2
87	2018	16.3	2.7	0.281202	0.000033	0.000893	0.281168	-56.0	1.2	-11.6
90	1721	13.5	2.2	0.281921	0.000037	0.000869	0.281893	-30.5	1.3	7.3
91	1788	28.1	2.6	0.281651	0.000032	0.001647	0.281596	-40.1	1.1	-1.7
95	576	1.3	3.1	0.282245	0.000038	0.000060	0.282244	-19.1	1.3	-6.3
96	1402	28.1	2.3	0.282070	0.000040	0.001567	0.282029	-25.3	1.4	4.8
97	515	18.7	2.7	0.282307	0.000024	0.001198	0.282295	-16.9	0.8	-5.9
98	699	14.7	2.0	0.282600	0.000027	0.000884	0.282589	-6.5	1.0	8.7
102	607	12.0	2.5	0.282436	0.000035	0.000736	0.282428	-12.3	1.2	0.9

**Table DR8. Hf isotope analyses for detrital zircons**

Spot	Age (Ma)	$(^{176}\text{Yb} + ^{176}\text{Lu}) / ^{176}\text{Hf}$ (%)	Volts Hf	$^{176}\text{Hf}/^{177}\text{Hf}$	$\pm$ (1s)	$^{176}\text{Lu}/^{177}\text{Hf}$	$^{176}\text{Hf}/^{177}\text{Hf}_{(t)}$	$\epsilon_{\text{Hf}(0)}$	$\pm$ 1s	$\epsilon_{\text{Hf}(t)}$
<b>Y2-MD092</b>										
2	799	19.3	3.0	0.282457	0.000032	0.001080	0.282441	-11.6	1.1	5.7
5	2740	37.2	3.3	0.280989	0.000032	0.002148	0.280876	-63.5	1.1	-5.2
9	1049	36.1	3.1	0.282386	0.000033	0.002198	0.282342	-14.1	1.2	7.9
10	1864	19.6	2.5	0.281583	0.000031	0.001227	0.281540	-42.5	1.1	-2.0
11	1031	13.6	2.7	0.282194	0.000031	0.000839	0.282178	-20.9	1.1	1.6
12	937	13.6	2.5	0.281880	0.000035	0.000826	0.281865	-32.0	1.2	-11.6
14	2565	4.1	3.3	0.281063	0.000026	0.000236	0.281052	-60.9	0.9	-3.0
18	1455	22.0	2.9	0.282025	0.000026	0.001347	0.281988	-26.9	0.9	4.5
21	525	10.7	3.2	0.282265	0.000030	0.000602	0.282259	-18.4	1.0	-6.9
23	1151	12.0	2.8	0.282245	0.000029	0.000712	0.282230	-19.1	1.0	6.2
27	480	35.8	2.3	0.282644	0.000035	0.002037	0.282626	-5.0	1.3	5.1
29	435	8.4	1.8	0.282135	0.000039	0.000476	0.282131	-23.0	1.4	-13.4
31	2830	17.6	3.6	0.280864	0.000032	0.000943	0.280813	-67.9	1.1	-5.3
32	585	7.6	2.6	0.282386	0.000030	0.000455	0.282381	-14.1	1.1	-1.2
38	570	2.9	2.9	0.282331	0.000035	0.000178	0.282329	-16.0	1.2	-3.4
41	1066	17.9	2.4	0.282305	0.000034	0.000960	0.282285	-17.0	1.2	6.2
43	1802	44.0	2.7	0.281579	0.000028	0.002587	0.281490	-42.7	1.0	-5.2
45	711	9.1	2.6	0.282246	0.000025	0.000554	0.282239	-19.1	0.9	-3.5
45A	711	60.6	2.3	0.282474	0.000054	0.004084	0.282420	-11.0	1.9	3.0
47	574	0.5	2.8	0.282367	0.000040	0.000029	0.282367	-14.8	1.4	-2.0
48	1057	29.2	2.4	0.282198	0.000028	0.001617	0.282166	-20.7	1.0	1.8
55	2019	22.9	2.8	0.281348	0.000030	0.001238	0.281301	-50.8	1.1	-6.9
57	1100	27.9	3.2	0.282255	0.000032	0.001542	0.282223	-18.7	1.1	4.8
60	1022	36.4	3.0	0.282248	0.000032	0.002066	0.282209	-19.0	1.1	2.5
62	557	1.1	2.7	0.282361	0.000026	0.000068	0.282360	-15.0	0.9	-2.6
63	551	34.4	2.7	0.282281	0.000037	0.001760	0.282262	-17.8	1.3	-6.2
67	953	20.5	1.9	0.282205	0.000047	0.001129	0.282185	-20.5	1.6	0.1
70	765	9.5	2.4	0.282242	0.000030	0.000541	0.282234	-19.2	1.1	-2.4
72	1763	8.4	3.0	0.281525	0.000029	0.000526	0.281507	-44.6	1.0	-5.4
73	2640	39.9	2.3	0.281190	0.000037	0.002263	0.281075	-56.4	1.3	-0.4
74	1726	6.4	3.1	0.281736	0.000022	0.000482	0.281720	-37.1	0.8	1.3
75	1028	8.6	2.2	0.282306	0.000030	0.000540	0.282296	-16.9	1.1	5.7
78	557	76.3	2.2	0.282493	0.000036	0.004576	0.282445	-10.3	1.3	0.4
79	1115	15.8	2.7	0.282280	0.000029	0.000973	0.282259	-17.9	1.0	6.4
81	599	0.8	2.9	0.282542	0.000024	0.000045	0.282542	-8.6	0.9	4.8
82	1816	10.9	2.2	0.281482	0.000027	0.000735	0.281456	-46.1	1.0	-6.0
83	541	1.0	2.7	0.282399	0.000030	0.000077	0.282398	-13.7	1.0	-1.6
85	488	4.6	2.6	0.282440	0.000033	0.000307	0.282437	-12.2	1.2	-1.4
86	622	10.4	2.5	0.282424	0.000032	0.000613	0.282417	-12.8	1.1	0.9
90	564	20.9	2.1	0.282070	0.000045	0.001381	0.282055	-25.3	1.6	-13.2
92	979	23.6	2.1	0.282418	0.000039	0.001619	0.282388	-13.0	1.4	7.9
94	3034	16.3	1.9	0.280714	0.000039	0.001013	0.280655	-73.2	1.4	-6.1
95	1027	14.2	2.1	0.282384	0.000038	0.000915	0.282366	-14.2	1.3	8.2
96	527	83.8	1.8	0.282459	0.000060	0.004933	0.282411	-11.5	2.1	-1.5
99	1746	11.9	2.3	0.281781	0.000030	0.000815	0.281754	-35.5	1.1	2.9
100	878	12.6	1.9	0.282257	0.000040	0.000939	0.282242	-18.7	1.4	0.4
103	1040	8.6	2.3	0.282332	0.000024	0.000509	0.282322	-16.0	0.8	6.9
104	1775	1.2	2.9	0.281607	0.000020	0.000075	0.281604	-41.7	0.7	-1.7
105	1254	10.5	2.3	0.282219	0.000031	0.000668	0.282203	-20.0	1.1	7.6

Notes:

 $^{176}\text{Lu}$  decay constant of  $1.867 \times 10^{-11}$  (Soderlund et al. 2004). $^{176}\text{Hf}/^{177}\text{Hf}$  and  $^{176}\text{Lu}/^{177}\text{Hf}$  CHUR values of 0.282785 and 0.0336 (Bouvier et al. 2008).





**Table DR9. Hf and O isotope analyses of zircons from granites**

spot	assigned age (Ma)	$^{18}\text{O}/^{16}\text{O}$	$\pm 10^{-7}$	$\delta^{18}\text{O} \text{‰}$	$\pm 2 \text{ S.E.}$	$^{176}\text{Hf}/^{177}\text{Hf}$	$\pm 10^{-6}$	$^{176}\text{Lu}/^{177}\text{Hf}$	$\pm 10^{-5}$	$\epsilon_{\text{Hf}(0)}$	$^{176}\text{Hf}/^{177}\text{Hf}_{(\text{l})}$	$\epsilon_{\text{Hf}(\text{l})}$	$\pm 2 \text{ S.E.}$
<b>C5-I51a (Yakymchuk et al., 2013)</b>													
1	353	0.0020490	6	9.57	0.36	0.282415	21	0.00103	10	-13.1	0.282408	-5.5	0.7
3	353	0.0020465	19	8.34	0.97	0.282591	26	0.00093	9	-6.9	0.282584	0.8	0.9
4	353	0.0020467	5	8.44	0.34	0.282509	30	0.00096	10	-9.8	0.282502	-2.1	1.1
7	1055	0.0020436	6	6.92	0.35	0.282221	41	0.00191	20	-19.9	0.282183	2.4	1.4
8	353	0.0020516	5	10.84	0.32	0.282498	34	0.00098	10	-10.1	0.282492	-2.5	1.2
9	353	-	-	-	-	0.282441	23	0.00106	11	-12.2	0.282434	-4.6	0.8
10	353	0.0020567	11	12.61	0.67	0.282492	30	0.00125	12	-10.4	0.282484	-2.8	1.1
12	353	0.0020566	16	12.58	0.88	-	-	-	-	-	-	-	-
13	353	0.0020565	5	12.53	0.47	0.282550	36	0.00048	5	-8.3	0.282547	-0.6	1.3
14	353	-	-	-	-	0.282479	27	0.00129	13	-10.8	0.282470	-3.3	1.0
<b>M5-G175 (Yakymchuk et al., 2013)</b>													
1.1	369	0.0020483	4	8.53	0.45	0.282565	27	0.00130	4	-7.8	0.282556	0.1	0.9
2.1	369	0.0020464	5	7.59	0.47	0.282386	22	0.00093	2	-14.1	0.282379	-6.1	0.8
2.2	630	0.0020403	5	4.63	0.48	-	-	-	-	-	-	-	-
3	369	0.0020458	4	8.75	0.28	0.282457	28	0.00160	3	-11.6	0.282446	-3.8	1.0
4	369	0.0020458	4	8.71	0.29	0.282463	50	0.00146	4	-11.4	0.282453	-3.5	1.8
5	369	0.0020437	4	6.26	0.46	0.282504	30	0.00115	2	-9.9	0.282496	-2.0	1.1
6	369	0.0020474	4	9.53	0.28	0.282570	78	0.00206	6	-7.6	0.282556	0.1	2.7
7	369	0.0020428	7	5.84	0.52	0.282569	30	0.00185	6	-7.6	0.282557	0.1	1.1
9	369	0.0020437	5	7.72	0.32	0.282544	21	0.00077	4	-8.5	0.282539	-0.5	0.7
10	369	0.0020462	3	8.95	0.24	0.282416	21	0.00104	2	-13.0	0.282409	-5.1	0.7
11	369	0.0020476	4	9.59	0.26	0.282403	40	0.00140	3	-13.5	0.282393	-5.7	1.4
15	369	0.0020420	3	6.85	0.25	0.282571	23	0.00102	1	-7.6	0.282564	0.4	0.8
16	369	0.0020459	3	8.77	0.25	0.282506	27	0.00110	4	-9.9	0.282498	-1.9	0.9

Notes:

 $^{176}\text{Lu}$  decay constant of  $1.865 \times 10^{-11}$  (Soderlund et al. 2004). $^{176}\text{Hf}/^{177}\text{Hf}$  and  $^{176}\text{Lu}/^{177}\text{Hf}$  CHUR values of 0.282785 and 0.0336 (Bouvier et al. 2008).

**Table S10. *p* values for Kruskal-Wallis test of zircon  $\epsilon\text{Hf}_t$  and  $\delta^{18}\text{O}$  distributions for pairs of Ford Granodiorite suite samples**

$\epsilon\text{Hf}$ (zircon)	MB.219	MB.214	M5-G175	Y1-IG071	Y2-JU096	51225-2	Y1-IG073	9N27-4	C5-Is51a	912-2A
MB.219	—	0.14	<b>0.00</b>							
MB.214	0.14	—	<b>0.00</b>							
M5-G175	<b>0.00</b>	<b>0.00</b>	—	<b>0.05</b>	0.43	0.76	0.31	0.81	0.76	0.68
Y1-IG071	<b>0.00</b>	<b>0.00</b>	<b>0.05</b>	—	<b>0.01</b>	0.06	0.07	<b>0.04</b>	0.09	<b>0.03</b>
Y2-JU096	<b>0.00</b>	<b>0.00</b>	0.43	<b>0.01</b>	—	0.29	<b>0.00</b>	0.28	0.19	0.77
51225-2	<b>0.00</b>	<b>0.00</b>	0.76	0.06	0.29	—	<b>0.02</b>	0.81	0.52	0.40
Y1-IG073	<b>0.00</b>	<b>0.00</b>	0.31	0.07	<b>0.00</b>	<b>0.02</b>	—	0.23	0.34	0.11
9N27-4	<b>0.00</b>	<b>0.00</b>	0.81	<b>0.04</b>	0.28	0.81	0.23	—	0.65	0.41
C5-Is51a	<b>0.00</b>	<b>0.00</b>	0.76	0.09	0.19	0.52	0.34	0.65	—	0.37
912-2A	<b>0.00</b>	<b>0.00</b>	0.68	<b>0.03</b>	0.77	0.40	0.11	0.41	0.37	—

$\delta^{18}\text{O}$ (zircon)	MB.219	MB.214	M5-G175	Y1-IG071	Y2-JU096	51225-2	Y1-IG073	9N27-4	C5-Is51a	912-2A
MB.219	—	0.13	<b>0.01</b>	<b>0.00</b>						
MB.214	0.13	—	0.12	<b>0.00</b>	<b>0.00</b>	<b>0.00</b>	<b>0.00</b>	<b>0.02</b>	<b>0.00</b>	<b>0.00</b>
M5-G175	<b>0.01</b>	0.12	—	<b>0.00</b>	0.16	<b>0.01</b>	<b>0.00</b>	0.38	<b>0.02</b>	0.53
Y1-IG071	<b>0.00</b>	<b>0.00</b>	<b>0.00</b>	—	<b>0.00</b>	0.06	0.10	<b>0.00</b>	0.48	<b>0.00</b>
Y2-JU096	<b>0.00</b>	<b>0.00</b>	0.16	<b>0.00</b>	—	<b>0.03</b>	<b>0.00</b>	<b>0.00</b>	<b>0.02</b>	0.53
51225-2	<b>0.00</b>	<b>0.00</b>	<b>0.01</b>	0.06	<b>0.03</b>	—	0.35	<b>0.00</b>	0.14	<b>0.00</b>
Y1-IG073	<b>0.00</b>	<b>0.00</b>	<b>0.00</b>	0.10	<b>0.00</b>	0.35	—	<b>0.00</b>	0.28	<b>0.00</b>
9N27-4	<b>0.00</b>	<b>0.02</b>	0.38	<b>0.00</b>	<b>0.00</b>	<b>0.00</b>	<b>0.00</b>	—	<b>0.00</b>	0.01
C5-Is51a	<b>0.00</b>	<b>0.00</b>	<b>0.02</b>	0.48	<b>0.02</b>	0.14	0.28	<b>0.00</b>	—	<b>0.03</b>
912-2A	<b>0.00</b>	<b>0.00</b>	0.53	<b>0.00</b>	0.53	<b>0.00</b>	<b>0.00</b>	<b>0.01</b>	<b>0.03</b>	—

For *p* values <0.05, the null hypothesis that the two groups sample the same population is rejected.